



1 Effects of Seasonal Snow Cover on Hydrothermal Conditions of the Active Layer in
2 the Northeastern Qinghai-Tibet Plateau

3 Ji Chen^{1,2}, Yu Sheng¹, Qingbai Wu^{1,2}, Lin Zhao³, Jing Li¹, Jingyi Zhao^{1,2}

4 ¹State Key Laboratory of Frozen Soil Engineering, Cold and Arid Regions Environmental and
5 Engineering Research Institute, Chinese Academy of Science, Lanzhou, 730000, China

6 ²Beiluhe Observation Station of Frozen soil Environment and Engineering, Cold and Arid
7 Regions Environmental and Engineering Research Institute, Chinese Academy of Science,
8 Lanzhou, 730000, China

9 ³Cryosphere Research Station on the Qinghai-Tibetan Plateau, Chinese Academy of Sciences,
10 Lanzhou, 730000, China

11 *Corresponding to:* chenji@lzb.ac.cn

12 **Abstract.** Snow cover significantly influences the moisture and thermal properties of the active
13 layer in permafrost regions. Seasonal snow cover, soil temperature, and moisture were monitored
14 in the northeastern Qinghai-Tibet Plateau (QTP) from December 2012 to February 2015.

15 According to field data, the following conclusions were drawn. (1) The snow season in this region
16 is predominantly during spring (March to May) and autumn (September to November), the
17 thickness of individual snowfall events is usually less than 5 cm, and the duration of land surface
18 snow cover is generally no longer than 5 days. (2) Removal of seasonal snow cover is beneficial
19 for cooling the active layer in a whole year and in other seasons with the exception of summer.

20 Further analysis on the ground temperature in the active layer shows that the cooling effect of the
21 snow removal maybe results from the high thermal resistivity of snow, the delay of snowfall time
22 in autumn, and the drastic decrease of moisture content in the active layer. (3) Seasonal snow
23 cover maintains the high water content of the active layer. Snow removal can therefore lead to a
24 rapid decrease of soil moisture content. A small decrease in water content of the active layer at the
25 natural snow site (NSS) is related with less rainfall during the monitoring period. Significant
26 differences between the NSS and the snow removal site (SRS) may depend predominantly on the
27 inhibitory action of snow cover on the evaporation capacity of surface soil because of its cooling
28 and shading effects during the daytime and in summer.

29 **Keywords:** Seasonal snow cover, Active layer, Soil temperature, Soil moisture, Qinghai-Tibet
30 Plateau



31 **1. Introduction**

32 The active layer is defined as the top layer of ground that is subject to annual thawing and
33 freezing in areas underlain by permafrost (Washburn, 1979). The active layer over permafrost
34 plays a significant role in the surface energy balance, the hydrologic cycle, carbon exchange
35 between the atmosphere and the land surface, ecosystems, landscape processes, and human
36 infrastructure in cold regions (Brown et al., 2000; Lemkeet al., 2007; Wang et al., 2009; Han et al.,
37 2010). Due to the impact of global climate change and human engineering activities, active layer
38 thickness and temperature have increased over the past few decades in the Arctic, Antarctic,
39 Alpine, QTP, and other areas (Brown et al., 2000; Jin et al., 2000; Zhao et al., 2000; Harris et al.,
40 2003; Nelson et al., 2004; Zhao et al., 2004; Wu and Liu, 2004; Zhang et al., 2005; Cheng and Wu,
41 2007; Zhao et al., 2008; Wu and Zhang, 2010; Zhao et al., 2010; Wu et al., 2012; Guglielmin and
42 Vieira, 2014).

43 Aside from the climate and human activities, changes in the active layer are strongly linked
44 to factors such as the physical and thermal properties of the surface soil, vegetation, soil moisture
45 content, and seasonal snow cover (Brown et al., 2000; Hinkel et al., 2003). Seasonal snow cover
46 has significant and complex effects on the hydrothermal regime of the active layer as a result of its
47 unique thermal properties. The high albedo of snow cover (98%) is helpful for reducing the snow
48 surface temperature. In high latitude areas, the average temperature of the nival surface in winter
49 is 0.5–2.0 °C lower than the air temperature (Weller, 1974; Yershov, 1998). The large latent heat
50 (335 kJ/kg) delays the snow cover thawing process and the ground heating rate by a significant
51 amount (Zhang, 2005). In addition, the evaporation of snow meltwater can also help to reduce the
52 land surface temperature. Good thermal insulation occurs in thick layers of snow because of the
53 small thermal conductivity coefficient of snow cover (0.15 W/m·k) (Zhang et al., 1996). However,
54 the thermal conductivity coefficient of snow cover is not fixed (Sturm et al., 1997). Monitoring
55 results from the Alps indicate that the increase rate of the snow cover thermal conductivity
56 coefficient is 0.01 W/m·k·d (Morin et al., 2010). A remarkable increase in this value, even by an
57 order of magnitude (Reimer, 1980), can be caused by the wind (Yen, 1965).

58 Dramatic spatio-temporal differences in the effects of snow cover on the active layer have
59 been observed due to the thermal properties mentioned above (Zhang, 2005). In high latitude areas
60 with thick snow cover, the temperature of both the active layer underneath the snow cover and the
61 permafrost is often significantly higher than that of bare land, with a 20 °C temperature difference
62 in some areas (Smith, 1975). In Alaska, ground temperatures at depths of 0.29 m and 3.0 m
63 dropped by 1.48 °C and 0.72 °C, respectively, when the snow cover thickness reduced from 40 cm
64 to 20 cm (Ling and Zhang, 2006). Daniel (2001) discovered that snow cover with a thickness
65 greater than 80 cm will have remarkable thermal insulation, and a decrease of 10 cm in snow
66 cover thickness can reduce the mean annual ground temperature (MAGT) by 0.3 °C. In the Amur
67 region of the Greater Khingan Mountains, snow cover 21–36 cm thick can increase the mean
68 annual ground surface temperature (MAGST) by 2.8–5.0 °C (Liang et al., 1993). In the Altai
69 Mountains in northwestern China, seasonal snow cover increases the temperature difference
70 between the ground surface and the atmosphere, which reaches 4.6–7.0 °C in the lower mountain
71 belt and 10°C in the medium mountain belt (Tong et al., 1986). In contrast with the thermal
72 insulation generally discovered in the Arctic Pole and the subarctic region, the effects of snow
73 cover on active layer temperature in the Antarctic Pole and mid-latitude regions are linked to snow
74 cover thickness. In the Antarctic continent, a cooling effect was observed when the snow cover



75 thickness was less than 0.6 m (Goyanes et al., 2014; Guglielmin et al., 2014). In mid-latitude areas
76 of the Alps, results from bottom temperature of snow (BTS) measurements indicate that 0.8 m is
77 the critical thickness for thermal insulation of the snow cover (Keller and Gubler, 1993), while
78 numerical simulation results show a critical thickness of 0.6 m (Luetschg et al., 2008). Jin et al
79 (2008) analyzed previous research data and proposed that, in eastern parts of the QTP, thermal
80 insulation occurs in seasonal snow cover when its thickness is more than 20 cm, which is similar
81 to monitoring results from the Qilian Mountain ice groove (Hao et al., 2009) and predictions using
82 the Coupmodel (Zhou et al., 2013). In addition, snow cover formation and thawing time can also
83 deeply influence the active layer temperature. Daniel (2001) analyzed the thermal regime of the
84 active layer over the Corvatsch site in the Alps and found that snow cover 5-15 cm thick in late
85 autumn could more effectively cool the shallow soil mass.

86 Snow cover influences not only the temperature and thickness of the active layer, but also the
87 soil moisture content. In spring, water content in the active layer increases remarkably, even
88 reaching saturation conditions, because of the infiltration of melted snow (Hinzman et al., 1991;
89 Hinkel et al., 2001). In winter, the permafrost shell thickness of the surface layer significantly
90 influences the infiltration of melted snow, while a permafrost shell more than 0.4 m thick could
91 impede infiltration (Iwata et al., 2011). Using observation results from high latitude areas, the
92 SNOW-17 snow cover energy and water balance model has been developed, which theoretically
93 discusses the effects of seasonal snow cover on the water content of the active layer (Anderson,
94 1976).

95 Previous studies have shown that seasonal snow cover remarkably influences the
96 hydrothermal regime of the active layer, producing significant spatio-temporal differences. In this
97 study, the western section of the Qilian Mountains in the northeastern QTP is investigated, where
98 mountain island permafrost dominates (Li et al., 2012; Li et al., 2014), and a wide distribution of
99 snow cover exists (Zeng et al., 1985; Chen et al., 1991). During the period from 2003 to 2010,
100 there has been a remarkable decrease in the number of average snow days and a gradual increase
101 in the stable snow cover (Sun et al., 2014). Because of differences in geographical location, the
102 area in this study differs significantly from the more commonly studied high latitude and Alpine
103 regions with respect to radiation, climate, and snow cover characteristics. Recent studies on snow
104 cover effects on the active layer in this area have mainly focused on numerical simulations and the
105 shallow soil layer at a depth of about 50 cm (Jin et al., 2008; Wang et al., 2011; Zhou et al., 2013;
106 Xiang et al., 2013). As the active layer thickness of the Qinghai-Tibet Plateau is usually 2-3 m
107 (Wu and Zhang, 2010), it is very difficult to objectively evaluate the effects of seasonal snow
108 cover on the hydrothermal regime of the active layer in this area without deep hydrothermal
109 monitoring.

110 **2. Description of Monitoring Site and Equipment**

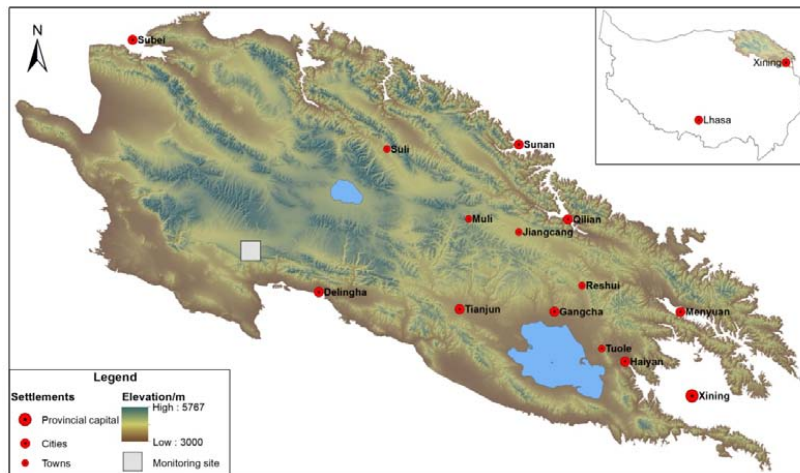
111 **2.1 Description of monitoring site**

112 The monitoring snow site, including the NSS and SRS, is located in the Yashatu basin of the
113 western Qilian Mountains in the northeast of Qinghai-Tibet Plateau, about 80 km from Delingha
114 city, Haixi Prefecture, Qinghai Province in the southeast and about 30 km from the Qaidam Basin
115 margin in the south, at 96.516° E and 37.6952° N (Fig.1a, b). The average altitude of this site is
116 approximately 4040 m. The snow site and its surrounding areas are flat with a maximal gradient of
117 0.5°. The Zongwulong Mountain, which runs nearly east to west at an altitude of 4500 m, is
118 located between the Yashatu basin where the snow site lies and the Qaidam Basin. There is a



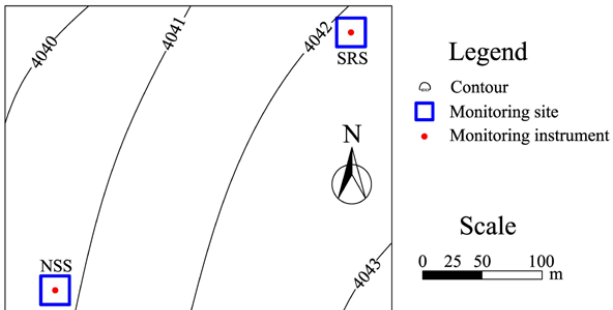
119 remarkable difference in the climate of Yashatu and Delingha city, attributed to influences of the
120 Zongwulong Mountain and the altitude contrast.
121

a. Site location



122

123 b. Layout of the NSS and SRS, and the positions of the instruments



124

125 c. Semi-desert landscape



d. Vegetation near the river



126

127 Figure 1 Location and layout of the NSS and SRS, the positions of the instruments, and typical
128 landscapes over the Yashatu basin in the Qilian Mountains, QTP

129 According to monitoring results from Yashatu Basin during the period from November 2009
130 to February 2015, the region has a minimum air temperature of -32.6 °C, a maximum air



131 temperature of 22.9 °C, an average annual temperature of -3.0-4.5 °C, an atmospheric pressure of
 132 610-630 hpa, and an annual precipitation of 100-200 mm. West, south, and southeast are the
 133 predominant wind directions in this area where the mean annual wind speed is 3.3 m s⁻¹ and the
 134 mean annual maximum half-hour wind speed is 18.3 m s⁻¹. Except for the two sides of the river
 135 where *Myricaria prostrata* and some *Koeleria tibetica* are found, other parts of the Yashatu Basin
 136 have vegetation coverage below 20%. Some areas even have bare surfaces, and describe typical
 137 half-desert or desert landscapes (Figure 1c and d).

138 According to drilling results from 2009 and pitting results from 2010, the depth of the active
 139 layer in the snow site is 3.0-4.0 m, mainly consisting of sandy soil, sandy-gravelly soil, gravelly
 140 soil, and mudstone. Mudstone is located 5.0 m below the NSS and 3.6 m below the SRS (Figure 2),
 141 where the total ice content is less than 10%. Based on a less than 0.1 °C standard temperature
 142 fluctuation, the annual ground temperature propagation depth of the snow site is less than 5.0 m,
 143 and the MAGT increased from -0.5 °C in 2009 to -0.4 °C in 2014. The MAGT at a depth of 15.0 m
 144 fluctuated between -0.32--0.30 °C during the period from 2009 to 2014, yet, due to the accuracy of
 145 the equipment and the probe, there has been effectively no change in ground temperature at a
 146 depth of 15.0 m over the past 4 years.

147 a-NSS

Site type	NSS		Longitude	96°31'	Latitude	37°42'	Vegetation cover	<20%
Total depth	15 m		Altitude	4040 m	Slope gradient	0.5°	Slope orientation	225°
Depth /m	Thick. /m	Column 1:100	Stratigraphic description				W.C.	Notes
0.6	0.6		Sandy-gravelly soil, earthy yellow, slight wet Sandy-gravelly soil, yellowish brown, gravel content equal to approximate 20%, water saturated Sandy soil, reddish, with a few silty clay sandwich, frozen, ice rich Silty sand, steel gray, slightly sticky, frozen, total ice poor except for several ice-rich soil layer Mudstone, red, very sticky, frozen, total ice content <10%, except for seldom ice-rich soil layer	0.5	5.5	In this graph, W.C. is derived from weight method and represents the mass water content in the active layer.		
				1.0	3.5			
				1.5	7.1			
				2.1	2.6			
				2.6	10.2			
				2.8	15.8			
				3.0	36.9			
4.3	1.3			4.7	30.0			
5.0	0.7			5.5	25.5			
6.0	1.0							

148

149 b-SRS

Site type	SRS		Longitude	96°31'	Latitude	37°42'	Vegetation cover	<10%
Total depth	50 m		Altitude	4043 m	Slope gradient	0.5°	Slope orientation	305°
Depth /m	Thick. /m	Column 1:100	Stratigraphic description				W.C.	Notes
0.4	0.4		Sandy soil with little gravel, yellowish brown Sandy loam with a lot of gravel, grayish yellow Gravelly soil, steel gray, proportion of rock with diameter > 2 cm is more than 30%, water saturated Sandy soil with a lot of gravel, gray, proportion of rock with diameter > 2 mm is about 20% Gravelly soil, steel gray, proportion of rock with diameter > 2 mm is about 60%, secondary psephicity; 2.7 m-3.0 m, water saturated, 3.0 m-3.5 m, moist; 3.5 m-3.6 m, frozen, ice poor Mudstone, red, very sticky, frozen, total ice content <10%, except for seldom ice-rich soil layer	0.3	2.9	In this graph, W.C. is derived from weight method and represents the mass water content in the active layer.		
0.8	0.4			0.8	6.5			
				1.5	10.4			
				2.5	10.4			
				3.5	27.8			
				4.0	31.6			

150

151 Figure 2 Lithological column based on test pit and borehole data from the NSS and the SRS



152 The field survey of the permafrost site in the Yashatu Basin was carried out in March 2009
153 and the borehole study was completed by the end of September. Ground temperature and
154 meteorological equipment was installed and used for monitoring by the end of November. Air
155 temperature and humidity were simultaneously monitored by CR3000 (HMP45C) and Hobo
156 (S-THB-M002). Two monitoring locations with a separation distance of approximately 300 m
157 were established by May 2010 (Figure 1b), the NSS and the SRS, which had similar ground
158 vegetation (Figure 1c) and lithologies (Figure 2) i.e. semi-desert landscape with sparse vegetation.
159 Monitoring results during the period of 2010-2012 indicated that the difference in mean annual
160 ground temperature between the two locations was less than 0.05 °C and the maximum snow
161 season was approximately 2 months.

162 The hydrothermal probe for the active layer was established by May 2010. Two sets of
163 monitoring devices were installed in the center of the two locations (Figure 1b) in order to perform
164 a comparative study on the effects of snow cover. In 2012, the two sets of monitoring devices were
165 upgraded. Surface albedo and surface infrared temperature probes were added to one site to
166 monitor the snow removal site, and probes for surface albedo, surface infrared degrees, ultrasonic
167 snow depth, and shallow soil thermal flux were added to the other set of equipment to monitor the
168 natural snow site. Detailed information on the type, model, properties, and quantity of the probes
169 is listed in Table 1.

170 Table 1 Characteristics of probes used at the Yashatu snow site. AT&H = Air temperature and
171 humidity, GST = ground surface temperature, SM = soil moisture, and ST = Soil temperature

Types	Versions	Accuracy	Ranges	Numbers		Brand	Notes
				SRS	NSS		
Wind	05103-L	$\pm 1 \text{ m s}^{-1}$	0-100 m s^{-1}	1	/	R.M. Young	/
AT&H	HMP45C	2% RH, $\pm 0.2^\circ\text{C}$ (20 °C)	0.8%-100% RH, -40 °C to +60 °C	1	/	Vaisala	/
	S-THB-M002	2.5% RH, $\pm 0.2^\circ\text{C}$ (+50 °C)	0%-100% RH, -40 °C to +75 °C	1	/	Hobo	/
Barometer	CS106	$\pm 1.5 \text{ mb}$	500-1100 mb	1	/	Vaisala	/
Rain gauge	TRWS 200E	0.1%	750 mm	1	/	MPS SYSTEM	/
Albedo-1	NR01	$<15 \text{ W m}^{-2}$	0-2000 W m^{-2}	1	/	Hukseflux	/
Albedo-2	240-8104	$<1 \text{ W m}^{-2}$	0-1500 W m^{-2}	/	1	Novalynx	/
GST	SI-111	$\pm 0.2^\circ\text{C}$	-40-70 °C	1	1	Apogee	/
Snow depth	260-700	$\pm 1 \text{ cm}$	0.5-10 m	/	1	NovaLynx Corporation	/
Thermal flux	HFP01	$50 \mu\text{V}/\text{W m}^{-2}$	-2000-+2000 W m^{-2}	2	2	Hukseflux	≈ 1
SM-1	CS616-L	$\pm 2.5\%$	0-100%	10	/	Campbell Scientific, Inc.	≈ 2
SM-2	SM300	$\pm 2.5\%$	0-50%	/	10	SPECTRUM	≈ 2
ST	SKLFSE-TS	$\pm 0.05^\circ\text{C}$	-30- + 30 °C	10	10	/	≈ 3

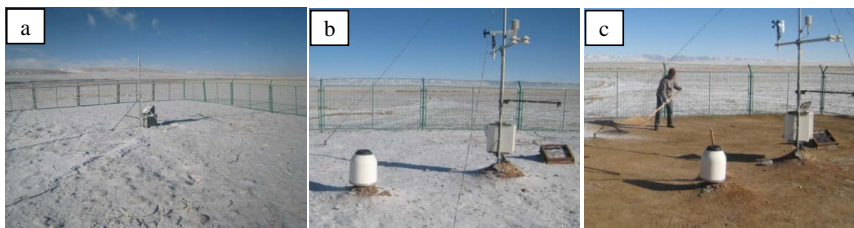
172 Notes: ≈ 1 : The heat flux plates are laid at depths of 5 cm and 10 cm. ≈ 2 : The soil moisture probes are laid at
173 depths of 5 cm, 20 cm, 40 cm, 80 cm, 120 cm, 160 cm, 200 cm, and 250 cm. ≈ 3 : The soil temperature probes are
174 laid at depths of 5 cm, 20 cm, 40 cm, 80 cm, 120 cm, 160 cm, 200 cm, 250 cm, 300 cm, and 400 cm.

175 The propagation rate of sonic waves was adjusted by using the existing temperature probe of
176 the monitoring site to enhance measurement accuracy of the snow depth. In the QTP, the snow



177 cover thickness of the shallow ground is usually less than 6cm, and the duration of snow cover is
178 generally 2-3 days (French, 2007). High frequency continuous data are needed to analyze the
179 effect of snow cover on the active layer because snow cover changes rapidly. In order to capture
180 the hydrothermal states of the active layer, all sensors including the infrared surface temperature
181 probe, the snow depth probe, and the surface albedo probe were connected to the CR3000
182 automatic data acquisition instrument with a half hour acquisition time interval. However, due to a
183 power supply problem that was not carefully considered when upgrading the meteorological
184 station, leakage in data acquisition often occurred during the night at the snow removal site.

185 There is more than one dominant wind direction in this area, and the dominant wind
186 directions differ between seasons. Snow fences were not adopted in the SRS. Snow shovels and
187 brooms were used to remove the snow cover of the SRS. Snow removal was typically completed
188 one day after snowfall. Images of NSS and SRS before and after snow removal are shown in
189 Figure 3.



190
191 Figure 3 Experiment sites of seasonal snow cover in the Yashatu Basin of Qilian Mountains, QTP.
192 a) NSS after snow fall, b) SRS after snow fall, and c) SRS after snow removal.

193 **2.2 Soil temperature acquisition**

194 The SKLFSE-TS probe manufactured under the supervision of the State Key Laboratory of
195 Frozen Soil Engineering (SKLFSE, China) was adopted to monitor soil temperature at the snow
196 site. The SKLFSE-TS thermistor temperature probe has been widely used since 1982 (Cheng,
197 1980), currently for permafrost engineering and environmental monitoring along the
198 Qinghai-Tibet railways (Cheng, 2005, 2007; Zhang et al., 2008; Wu and Zhang, 2008; Zhao et al.,
199 2010). The thermistors calibration is also carried out through comparison with the national
200 second-class platinum resistance thermometer in a temperature calibration tank. Detailed
201 calibration process and method are described in the study of Liu et al. (2011). The measuring
202 range of the SKLFSE-TS temperature probe is -30 °C+30 °C, which can be extended to ±40 °C
203 when standardization is performed under wide temperature ranges. The temperature resolution is
204 0.01 °C, temperature accuracy is ±0.05 °C, and the cable is longer than 300 m (Shen et al., 2012).

205 **2.3 Soil moisture acquisition**

206 The CS616 sensor manufactured by Campbell Scientific INC. U.S.A. was adopted for soil
207 moisture monitoring. The probe has two extensions 300 mm long, 3.2 mm in diameter, and with a
208 32 mm separation distance. Based on the principle of FDR (Frequency Domain Reflector), CS616
209 can only be used to measure the volumetric water content in soil (Campbell Scientific Inc., 2004).
210 All water contents mentioned in this paper are volumetric water contents, except for some special
211 cases, discussed below.

212 Unlike the temperature probes, the soil moisture probes have to be laid in layers by digging a
213 test pit, instead of being laid by drilling. Considering the convenience of construction, the soil
214 moisture monitoring probes are usually laid when the active layer reaches maximum thawing



penetration. Previous research results indicate that the active layer in permafrost regions in the Qinghai-Tibet Plateau usually reaches the maximum thawing penetration in September and October (Wu and Zhang, 2010). The water probes were due to be installed in October 2009. However, it was found during drilling in September of 2009 that sandy soil and gravelly soil occupied most of the depth from 0-3.6 m where the underground water level was less than 1.0 m. As a result, the water probes were unable to be laid. The probes were finally laid in May 2010 when the active layer was completely frozen and no longer melting. The water probes were laid at 5, 20, 40, 80, 120, 160, 200, and 250 cm depth from the surface. Comparative monitoring of the snow cover over the two locations started in December 2012. Because the hydrothermal probes had been installed in the active layer by 2010, digging of the active layer wouldn't significantly influence the accuracy of monitoring data after December 2012.

The CS616 probe only measures water content in the thawing soil and unfrozen-water content in the frozen soil (Kunio Watanabe and Tomomi Wake, 2009; Gary Parkin et al., 2013). When the active layer is frozen, measurement results are much lower than the true value. In order to discuss the true water content and its variability, only values measured in the thawing period were analyzed in this paper.

3. Monitoring results

3.1 Characteristics of snow cover in the Yashatu Basin

Field observations and automatic data collected from the meteorological data for the period from December 2012 to October 2014 indicate that the MAAT, maximum and minimum temperature are -3.4, 15.4 and -26.5 °C, respectively, and the mean annual relative humidity is 32.8% (Figure 4). For the same period there are 45 measured snowfalls in the Yashatu Basin, with a total surface snow cover thickness of 69.3 cm, and a 2-year accumulated surface snow cover duration of 77 days.

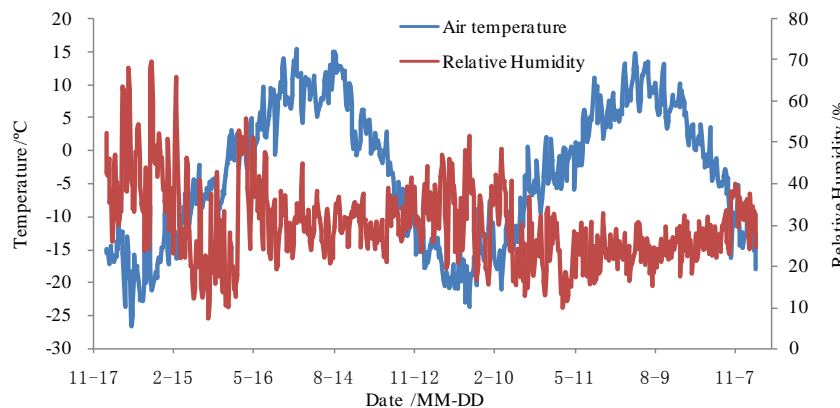
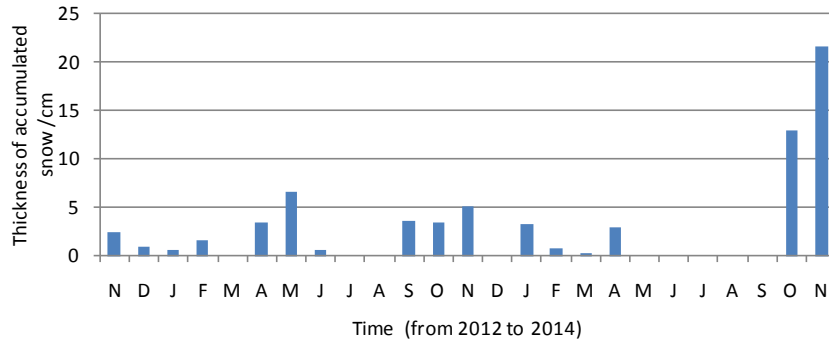


Figure 4 Variation in air temperature and relative humidity from 2012.12 to 2014.11

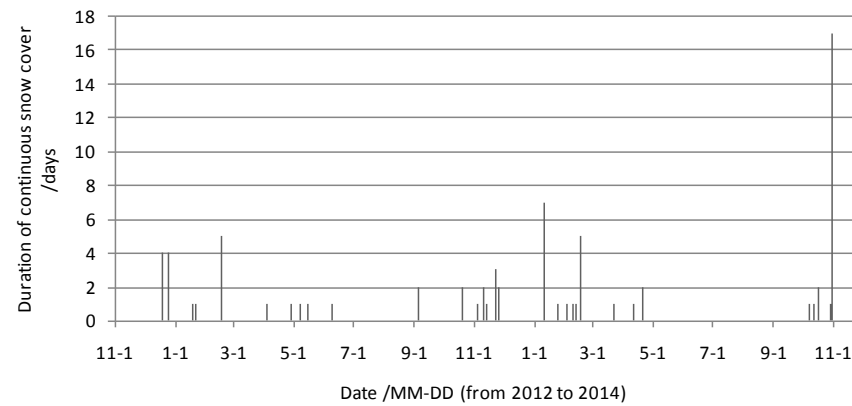
During the 2-year monitoring period, the distribution of snow cover is highly uneven and changes significantly between months and years (Figure 5). Over the period from December 2012 to November 2013, snowfall occurs in all months except for March, July, and August. The accumulated annual snow cover is 25.5cm, the mean monthly accumulated snow cover is about 2cm, and the maximum monthly snow cover is 6.7cm. From December 2013 to November 2014, snow falls only in six months, mainly in October and November. For 2014-10-30 to 2014-11-15,



247 the accumulated snow cover thickness is 29.4 cm, and snowfall occurs 15 times. Compared with
248 the previous year, the accumulated snow cover thickness increases by 18.3 cm in 2014.



249
250 Figure 5 Monthly accumulated snow cover thickness from 2012 to 2014 in the Yashatu Basin
251 After each snowfall in the Yashatu Basin, the duration of surface snow cover is generally less
252 than 5 days (Figure 6), and the average melting time of each snowfall is less than 2.5 days, while
253 the snow cover duration is typically less than one day. During the period from the end of October
254 to the middle of November 2014, due to low temperatures and more than ten snowfalls, the
255 duration of surface snow cover increases to 17 days, which is the longest continuous snow cover
256 event in the Yashatu Basin over the two years.



257
258 Figure 6 Timing of snowfall and duration of continuous snow cover events from 2012 to 2014 in
259 the Yashatu Basin

260 Snowfall in the Yashatu Basin shows significant seasonal differences (Table 2). In winter
261 (December–February), the accumulated snow cover thickness is not large, but the duration of snow
262 cover is long because of low air temperatures. Conversely, in spring (March–May), the
263 accumulated surface snow cover thickness is large and the snow cover duration is short because of
264 enhanced surface radiation and increasing air temperatures, and the melting time of single snow
265 cover events is usually less than one day. In summer (June–August), the accumulated snow cover
266 has the lowest thickness, and the melting time is usually within several hours. In autumn
267 (September–November), the accumulated snow cover is thickest, and the surface snow cover
268 duration is the longest.



269

Table 2 Accumulated thickness and days of snow cover over four seasons in the Yashatu Basin

Start and end time	2012.12-2013.11		2013.12-2014.11		
	Seasons	Thickness (cm)	Duration (days)	Thickness (cm)	Duration (days)
Winter (12-2)		3.1	15	5.6	16
Spring (3-5)		10.2	4	3.0	5
Summer (6-8)		0.6	1	0.0	0
Autumn (9-11)		12.1	13	34.7	22

270

3.2 The active layer thickness (ALT) and soil temperatures in the active layer

271

According to the definition of Muller (1947), the active layer floor is usually equal to the maximum seasonal depth of the 0 °C isotherm. This definition has been widely recognized and accepted because it eliminates various field interferences to the freezing-thawing depth, which is helpful to perform quantitative analysis on ALT (Brown et al., 2000). The thawing and refreezing process curves in the NSS and SRS during the period of 2013.3-2014.12 are given in Figure 7 based on the ground temperature monitoring data during the period of 2013.3.1-2014.2.28. As shown in figure 7, the ALTs of the two sites are 339.1cm and 340.6 cm in 2013, and 360.5 cm and 363.4 cm in 2014. Accordingly, the ALTs in the two sites have increased by 21.4 cm and 22.8 cm respectively.

272

273

274

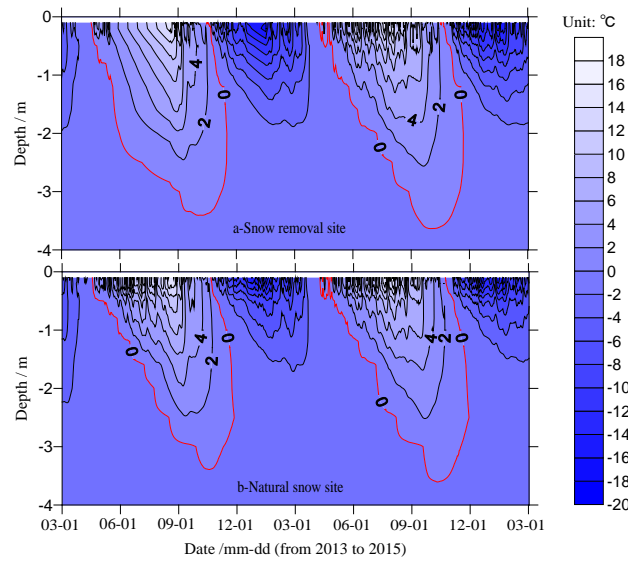
275

276

277

278

279



280

281

Figure 7 Ground temperature regime in the NSS and the SRS

282

283

284

285

286

287

288

The soil temperature of the active layer, especially the topsoil, changes greatly throughout the year (Figure 7). It is therefore unsuitable to estimate the thermal effect of seasonal snow cover on the active layer by comparing the ground temperature at one point in time. The mean annual soil temperature is the average value of soil temperatures acquired at a certain frequency in one year, which synthetically reflects the thermal regime of soil at any depth in the active layer, or in a perennial frozen earth layer, and can be used to study trend of the thermal regime of the active layer or permafrost (Wu and Zhang, 2008).

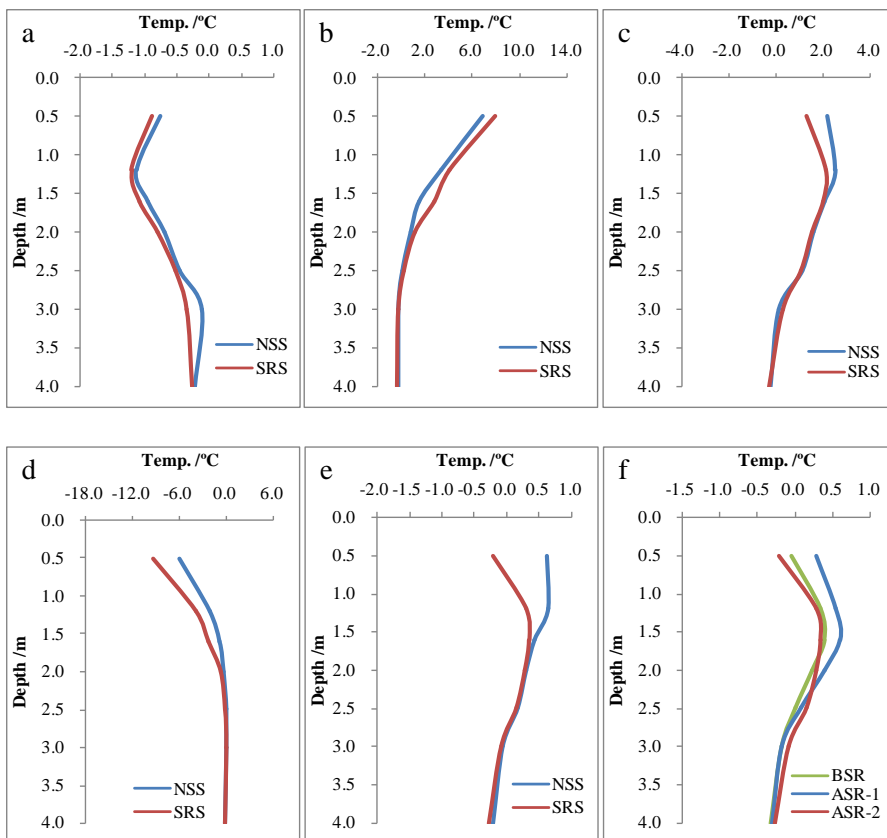
289

290

Previous studies suggest that the daily geothermal propagation depth is within 2.0 m (Yershov, 1998). In the QTP, we assume that the depth, where daily soil temperature amplitude is less than



291 0.1 °C, is the daily geothermal propagation depth. Excluding the daily meteorological extremes
 292 and the effect of human activities, the daily geothermal propagation depth in the quaternary strata
 293 is usually less than 0.5 m. The soil temperature of layers above 0.5 m depth varies significantly
 294 within one day, and it is not sufficient to obtain the average daily soil temperature of layers at 0.05
 295 m and 0.20 m depth by acquiring ground temperature at a single time, several times, even partial
 296 time of each day. Continuous monitoring data of the SRS at night could not be acquired most of
 297 the time, therefore the true mean annual soil temperature at depths of 0.0 m, 0.05 m, and 0.20 m in
 298 the SRS can also not be determined. The profile of average soil temperature versus depth for
 299 different seasons and over one year only at 0.5 m depth and below in the NSS and SRS from
 300 2014.3.1-2015.2.28 is shown in Figure 8. The mean annual temperature profile of the SRS before
 301 and after snow removal is also shown in Figure 8f.
 302



303
 304 Figure 8 Mean annual soil temperature profile of active layers in the NSS and SRS, where a, b, c,
 305 d, and e refer to the average soil temperatures within the active layers of the two sites in spring
 306 (March-May), summer (June-August), autumn (September-November), winter
 307 (December-February), and the entire year. Panel f shows the mean annual soil temperature at the
 308 SRS before and after snow removal. NSS and SRS refer to natural snow site and snow removal
 309 site, respectively. BSR means before snow removal in the SRS (2011.12-2012.11), and ASR refers
 310 to after snow removal. ASR-1 and ASR-2 indicate the first (2012.12-2013.11) and second



311 (2013.12-2014.11) years after the start of snow removal, respectively.

312 In spring, the soil temperature of the active layer in the NSS is higher than that of the SRS,
313 with a temperature difference of generally less than 0.1 °C, except for the area near 3 m depth
314 (Figure 8a). In summer, the temperature of the NSS at 0.5-2.0 m depth is about 1 °C lower than
315 that of the SRS, while at 2.5-4.0 m depth, the temperature of the two sites is almost the same
316 (Figure 8b). In autumn, the temperature of the NSS at 0.5-1.5 m depth is approximately 0.5 °C
317 higher than that of the SRS, and at depths below 1.5 m, the temperature difference of the two sites
318 is less than 0.1 °C (Figure 8c). In winter, the temperature of the NSS at 0.5-2.0 m depth is at most
319 3.3 °C higher than the SRS, while at depths below 2.0 m, the temperature curves of the two sites
320 are basically equal, and the maximum temperature difference is no more than 0.1 °C (Figure 8d).
321 Ground temperature at all depths in the active layer is higher in the NSS than that in the SRS with
322 exception of summer. Their difference decreases with the depth.

323 In terms of yearly temperature, the mean annual soil temperature difference in active layers
324 of the two sites also decreases with an increase in depth, and the temperature difference at 0.5 m
325 depth is the greatest, with the NSS being 0.8 °C warmer than SRS. From 1.6 m to the bottom of
326 the active layer, ground temperatures are all higher in the NSS than that in the SRS. However, the
327 mean annual soil temperature difference of the two sites is generally less than 0.3 °C (Figure 8e).

328 Temperature differences are observed in the active layer of the SRS before and after snow
329 removal (Figure 8f). In the first year after snow removal, increases of 0.3 °C and 0.2 °C occur at
330 depths of 0.5 m and 2.0 m, respectively. In the second year after snow removal, the temperature of
331 the active layer at 0-2.0 m depth decreases. Compared to the first year, decreases of approximately
332 0.5 °C and 0.1 °C at depths of 0.5 m and 2.0 m are observed, respectively. From 2012 to 2014, the
333 mean annual air temperature of Yashatu is -4.5 °C, -3.4 °C, and -3.9 °C, indicating that changes in
334 shallow soil temperature follow changes in air temperature during the monitoring period, namely,
335 by increasing and then decreasing.

336 **3.3 Soil moisture in the active layer**

337 The moisture profiles of the NSS and SRS from 2013.3.1 to 2015.2.28 are shown in Figure 9.
338 During the period from June-October, soil water content is 10-20% in the shallow soil, 0.2-0.5 m
339 depth, less than 10% at 0.4-0.7 m depth, and 20-40% beneath a depth of 0.4-0.7 m. Compared to
340 the NSS, there is more soil with low water content in the shallow layer and more soil with high
341 water content in the middle and bottom layers.

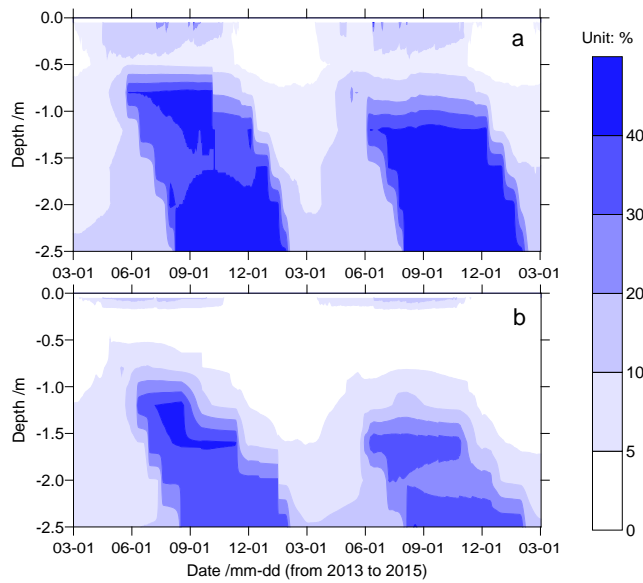
342 In October, with maximum thawing penetration, water content based on CS616 can reflect
343 the true soil moisture. From October 2013 to October 2014, soil moisture is redistributed in the
344 active layer and a change of total water content is not apparent in the NSS (Figure 9a), whereas
345 very large changes occur in the SRS (Figure 9b). Soil layers with water contents of more than 70%
346 have disappeared and areas with water contents between 30-40% have significantly reduced.

347 In order to perform quantitative analysis on soil moisture changes in the active layers of the
348 two sites, moisture content of various layers from the NSS and SRS during maximum thawing
349 penetration in 2012, 2013, and 2014 are shown in Figure 10.

350 At a depth of 0-50 cm, the range of soil moisture content in the two sites is no more than 4%,
351 and there are no significant changes during the 2012-2014 period. At a depth of 80 cm, soil
352 moisture decreases with time, and soil moisture in the NSS gradually decreases from 40.0% to
353 18.4% to 16.1%, while soil moisture in the SRS decreases from 34.4% to 4.8% to 4.5%. At depths
354 up to 120 cm, soil moisture in the NSS increases, the maximum annual increase in soil moisture of



355 each layer is less than 3%, and the increase over the two years is less than 4%. The change in soil
 356 moisture at depths below 120 cm in the SRS differs greatly from that of the NSS. At 120 cm depth
 357 the soil moisture gradually decreases from 31.5% to 9.2% to 7.2% and the soil moisture at 160 cm
 358 and 200 cm depth first increases then decreases, while the soil moisture at 250 cm depth increases.



359
 360 Figure 9 Volumetric moisture content based on the CS616 in (a) the NSS and (b) the SRS from
 361 2013.3.1 to 2015.2.28

362 Soil moisture content in the active layer changes significantly with depth, so simply comparing
 363 the soil moisture at a certain depth is not helpful for understanding the effects of seasonal snow
 364 cover on soil moisture in the active layer. The CS616 probe acquires the volumetric water content,
 365 under the assumption that the moisture content between the probes changes according to a known
 366 law, and therefore the average moisture content within the monitoring scope can be directly
 367 acquired from on site monitoring data. Referring to the acquisition method of the 0 °C isotherm,
 368 the linear interpolation method is used in this paper to obtain soil moisture content at various
 369 depths, and the overall moisture content of the active layer can be obtained through the following
 370 Eq. (1):

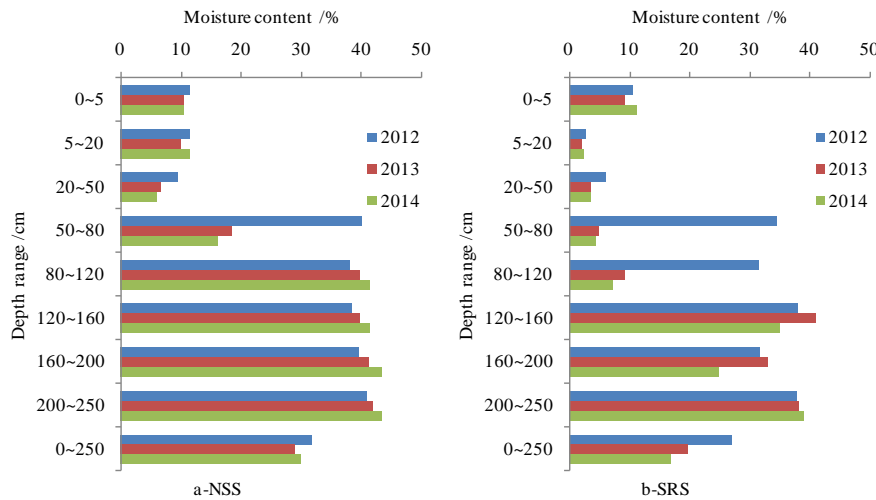
$$371 w = \left[H_1 \times w_1 + \sum_{i=2}^n (H_i - H_{i-1}) \times \frac{w_i + w_{i-1}}{2} \right] / H_n \quad (1)$$

372 In the above Eq. (1), the moisture content at 0-5 cm depth is the same as that at a depth of 5 cm,
 373 w and n refer to the average moisture content within the monitoring scope and the total number
 374 of probes in the active layer, respectively, H_i and w_i are the depth and moisture content of the
 375 i^{th} probe from top to bottom, and H_n is the depth of the probe at the n^{th} soil layer. The unit for
 376 H_i and H_n is cm, and % for w and w_i .

377 The overall moisture content of active layers in the two sites between 0-2.5 m depth at the
 378 maximum thawing penetration in 2012, 2013, and 2014 is obtained according to this method, and
 379 the calculation results are listed in Figure 10. From 2012 to 2014, the range in overall moisture
 380 content within the active layer at the NSS is 2.7%, and an accumulated decrease of 1.8% is



381 observed over the two years. The moisture content in the SRS decreases with time, with
 382 decreases of 7.3% and 2.7% observed in 2013 and 2014, respectively, and a total decrease of 10.0%
 383 over the two years. The overall moisture content within the active layer of the SRS has decreased
 384 by 8.2% more than in the NSS.



385
 386 Figure 10 Soil moisture content versus the depth in the active layer in the Yashatu Basin from
 387 2012 to 2014

388 4. Discussion

389 4.1 Could thin seasonal snow cover warm the active layer?

390 Whether in mid-latitude mountainous areas like the Alps(Keller and Gubler, 1993; Luetschg
 391 et al., 2008; Beniston et al., 2011; Tobias Rodder and Christof Kneisel, 2012), in high latitude
 392 areas such as the South Pole (Guglielmin et al., 2014; Goyanes et al., 2014), or in the
 393 Qinghai-Tibet Plateau (Jin et al., 2008; Hao et al., 2009; Zhou et al., 2013), snow cover with a
 394 thickness of <0.2 m usually has a net cooling effect, which helps to decrease the temperature of
 395 the active layer. The maximum snow cover thickness of Yashatu Basin during the period of
 396 2012.11-2014.11 is only 5 cm (Figure 5), which is much less than the previously determined
 397 critical snow cover thickness of 20 cm. Based on previous studies and monitoring results of snow
 398 cover thickness, a thin seasonal snow cover should decrease the temperature within the active
 399 layer at Yashatu sites. The ground temperature in the SRS should increase after snow removal.
 400 However, in reality, air temperature during the two consecutive years was higher than prior to
 401 snow removal the thickness of the snow cover was smaller than the critical snow cover thickness,
 402 and the average soil temperature of the active layer in the SRS two years after snow removal was
 403 lower than both before snow removal and the NSS.

404 The temperature decrease within the active layer of the SRS may be connected to the high
 405 thermal resistivity of snow cover, which decreases the heat dissipation intensity of the active layer
 406 in the winter (Goodrich, 1982; Sturm et al., 1992). The temperature decrease in the SRS may also
 407 be connected to the timing of snowfall. The observation and simulation results from Alaska
 408 indicate that the timing of snowfall influences the temperature within the active layer. A delay of
 409 10 days in snowfall time may result in a drop of 9 °C in surface temperature, which decreases by



410 1.1 °C at a depth of 2 m (Ling and Zhang, 2003). The main snowfall season in the Yashatu Basin is
411 in autumn (Figure 5), and the duration of surface snow cover is quite long (Figure 6). The cooling
412 period of the active layer is also in autumn, when the snow cover significantly decreases heat
413 release and hinders the temperature decrease within the active layer. The increase in ground
414 temperature under snow cover occurs not only in winter, but also throughout the whole year, when
415 the ground temperature may be higher (Williams, 1989). In fact, except for summer (Figure 8b),
416 the shallow soil temperature within the active layer of SRS is lower than that in the NSS in spring,
417 autumn, and winter (Figures 8a, 8c, and 8d).

418 Table 3 Average monthly thermal flux (W m^{-2}) at 5 cm depth from 2015.4-2016.3

Year	2015											2016		
	Month	4	5	6	7	8	9	10	11	12	1	2	3	
NSS		8.7	11.0	12.7	16.5	9.1	1.8	-4.2	-9.3	-14.0	-12.8	-7.5	0.9	
SRS		13.3	13.4	11.6	16.8	13.3	1.6	-4.7	-14.7	-20.5	-17.0	-6.4	2.5	

419 Note: In this table, positive number represents the thermal influx in the active layer. Negative numbers mean that
420 the active layer released its heat towards the atmosphere.

421 Soil moisture content in the active layer of the SRS has decreased continuously since snow
422 removal experiment began in December 2012 (Figure 10), which not only influences the
423 thawing-freezing process but also alters the thermal balance of active layer. The decrease of
424 moisture content influences the thermal balance in both areas. Firstly, the thermal conductivity
425 decreases, especially in the frozen state, which impedes the thermal release in winter and warms
426 the active layer. Secondly, decrease of moisture content releases the huge latent heat, which may
427 be the thawing latent heat or the evaporating latent heat. The thawing latent heat is 335 kJ kg^{-1} and
428 the evaporating latent heat is 2257 kJ kg^{-1} at 100°C under the condition of a standard atmospheric
429 pressure. The thawing and evaporating latent heat for the water with VWC equal to 1% in 1 m^3
430 soil body is 3350 kJ and 22570 kJ, respectively. When the average thermal capacity in the active
431 layer of the SRS is assumed to be $2267 \text{ kJ/(m}^3\cdot^\circ\text{C)}$ and the VWC decreases by 1%, the temperature
432 of the active layer can decrease by 1.5°C due to the thawing latent heat and 10.0°C due to the
433 evaporating latent heat theoretically. Therefore, the dramatic decrease in moisture content may be
434 the other significant factor which leads to the temperature decrease of the active layer in the SRS.

435 In order to verify this phenomenon, the problems experienced with the power supply were
436 solved at the SRS in April 2015. Thermal flux data were successfully collected at half-hour
437 intervals during the period from April 2015 to March 2016, and listed in Table 3. According to this
438 data, thermal states of the active layer can be classified into four stages: (a) warming stage
439 (April-August), (b) the first steady stage from warming to cooling (September), (c) cooling stage
440 (October-February), and (d) the second steady stage from cooling to warming (March). Excluding
441 February, heat release from the active layer in the NSS is less than that in the SRS during the
442 cooling stage. Excluding June, active layer heat intake is also less in the NSS than the SRS during
443 the warming stage. Abnormal heat fluxes in February and June are both related to significant
444 snowfall from October to January and from April to May, which leads to less heat release and heat
445 intake in the NSS than the SRS. Therefore, in February and June, when there is little or no
446 snowfall, the heat exchange is much greater in the NSS than in the SRS. During the period from
447 April 2015 to March 2016, the average thermal influx at 5 cm depth is 1.1 W m^{-2} in the NSS and
448 0.7 W m^{-2} in the SRS. Owing to the higher thermal intake, the average soil temperature of the
449 active layer is higher in the NSS than the SRS.



450 **4.2 What leads to the soil moisture decrease and disparity between the NSS and SRS?**

451 In permafrost areas, the active layer is the soil layer where soil moisture changes are most
452 active. Runoff on the surface and in the active layer, soil properties, as well as evaporation and
453 infiltration, can all alter the soil moisture content of the active layer. As the snow site is located in
454 the bottom of Yashatu Basin where the slope gradient is less than 1°, runoff here can be
455 disregarded because of the flat ground (Neal, 1938). In the process of installing soil moisture
456 probes, digging often changes the soil properties, such as soil structure, grain size distribution, and
457 compactness, etc. Grain size distribution is disturbed vertically and horizontally. However, the soil
458 in the active layer of the NSS and SRS is unstructured coarse sand and gravelly soil with inferior
459 water retention ability. The pit is fully backfilled layer-by-layer with the original soil according to
460 the excavation sequence in May. There is no significant difference between the pit surface and
461 neighboring ground surface in September, including the elevation and other surface characteristics.
462 It shows that the digging's influence on the soil moisture could be ignored in this field site.
463 Permafrost and mudstone, developed below the active layer, are often regarded as an impermeable
464 soil layer. Therefore, the contribution of downward seepage throughout the mudstone-permafrost
465 layer to soil moisture in the active layer is very small (Fetter, 2000).

466 The accumulated liquid precipitation in the Yashatu Basin during the period of
467 2012.12.1-2014.11.30 was 175 mm, and the accumulated surface snow cover thickness was 690
468 mm. According to previous results, the snow cover density in the Qilian Mountain area was 0.16 g
469 cm⁻³ (Hao et al., 2009), and the snow water equivalent (SWE) of two-year snow cover was 110
470 mm. Considering the liquid and solid precipitation quantities, the total precipitation in the Yashatu
471 Basin during the period of 2012.11-2014.11 was 285 mm. According to the observation results
472 from the neighboring Delingha meteorological station, annual rainfall in the urban area of
473 Delingha is 140 mm, and the evaporation reaches 2230 mm (Lv, 1960). The altitude in Yashatu
474 Basin is 1000 m higher than that of Delingha meteorological station, and according to rainfall
475 trends in mountain areas, the annual rainfall of the former should be larger than that of the latter.
476 In fact, the rainfall in Yashatu Basin during the period of 2012.12-2014.11 was similar to that of
477 Delingha. The rainfall in Yashatu for the year 2013 was only 100 mm, which is even less than that
478 of the urban area in Delingha. The analysis shows that Yashatu Basin experienced a significant dry
479 period in the years 2012-2014. Intense evaporation reduced the water supply from rainfall to the
480 active layer during these dry years, and finally resulted in the slight decrease in moisture content
481 observed in the NSS.

482 The SRS is influenced by both the dry years and the lack of snow cover compared to the NSS.
483 The SWE of snow in this area over the two years was 110 mm. This result could only increase the
484 moisture content at depth range of 0-2.5 m in the active layer by 4.4% at most, which is
485 significantly less than the 8% moisture content difference between the two sites. Therefore,
486 infiltration of melted snow cover alone cannot sufficiently explain this difference in moisture
487 content.

488 Infiltration is not the only way that the seasonal snow cover influences the moisture content
489 of the active layer, and the effect of snow cover on evaporation maybe more significant. Firstly,
490 the snow cover has a shielding effect on the surface. By coating the surface, the snow cover
491 changes the contact pattern between the atmosphere and the surface, and greatly reduces the effect
492 of airflow on surface soil evaporation (Penman, 1948; Yeh, 1983). Secondly, the shielding effect
493 of snow cover also significantly reduces surface warming from solar radiation. Compared to the



494 bare surface, the albedo of snow cover is high, and the snow surface temperature is even lower
495 than the air temperature (Yershov, 1998), and much lower than the bare surface. Therefore, the
496 ground surface temperature under the snow cover is lower than that of the SRS during the day or
497 in summer because of the low snow surface temperature. Furthermore, Yashatu Basin is located in
498 the mid-latitude zone, where the annual solar global radiation is fairly strong. Even in winter, solar
499 radiation greatly increases the temperature of the bare surface during the daytime. The monitoring
500 results from the west of Qilian Mountain indicate that the evaporation capacity of the surface soil
501 is enhanced by an increase in surface temperature (Wang and Guo, 2013). Additionally, the heat
502 needed for snow cover thawing comes not only from radiation from the sun and the surrounding
503 atmosphere, but also from the underlying surface soil, which helps to decrease the surface
504 temperature and reduce the evaporation capacity of the active layer.

505 Influenced by the reduction in precipitation and snow removal, moisture content within the
506 active layer in the SRS decreases significantly and consistently over the two years of this study.
507 Compared to the first year, the range of moisture content decreased in the second year by over
508 50%. The rate of moisture content decrease in the SRS will drop year by year as the snow removal
509 duration increases, until a new dynamic equilibrium is reached.

510 **5. Conclusions**

511 Based on analysis and discussion on the monitoring data from the monitoring sites of Yashatu
512 Basin in the western Qilian Mountain, Qinghai-Tibet Plateau, during the period of
513 2012.12.1-2015.2.28, some preliminary conclusions are drawn.

514 1. In Yashatu Basin, the snow cover is usually less than 5 cm, which can be classified as thin
515 snow cover. The annual accumulated snow cover thickness is usually less than 50 cm. The surface
516 snow cover duration is less than 5 days, which can be classified as short-term surface snow cover.

517 2. Over a calendar year, the ground temperature in the active layer is higher in the NSS than
518 that in the SRS. Seasonally, the ground temperature in the active layer is also higher in the NSS
519 than that in the SRS in other seasons with exception of summer. This phenomenon may result
520 from the high thermal resistivity of snow, snowfall time, and the marked decrease of moisture
521 content in the active layer.

522 3. Reduction of moisture content in the active layer of the NSS and SRS is related with less
523 rainfall and intensive evaporation during the period of 2012.12-2014.11. The dramatic decrease of
524 moisture content in the active layer of the SRS maybe depends on the removal of seasonal snow
525 cover.

526

527 **Acknowledgments**

528 This work was financially supported by the National Basic Research Program of China
529 (Grant No.2013CBA01803), the National Natural Science Foundation of China (Grant No.
530 41101065), and CAS “Equipment Development Project for Scientific Research” (Grant No.
531 YZ201523). Thanks to Honglian Chen and the Editage group (<http://online.editake.cn/dashboard>)
532 for English language editing.

533 **References**

- 534 Anderson, E.A.: A point energy and mass balance model of a snow cover, NOAA., Technical
535 Report NWS, 19, pp.150, 1976.
536 Brown, J., Hinkel, K. M. and Nelson, F. E.: The Circumpolar Active Layer Monitoring (CALM)
537 Program: Research design and initial results, Polar Geogr., 24(3), 165-253,



- 538 doi:10.1080/10889370009377698, 2000.
539 Campbell Scientific Inc.: CS616 and CS625 water content Reflectometer instruction manual,
540 Campbell Scientific Inc., Logan, UT, pp.2, 2004.
541 Chen, Q., and Chen, T.Y.: Climatical Analysis of Seasonal Snow Resources in Qilian Mountain,
542 Geographical Research, 19(1), 24-38, 1991(in Chinese).
543 Cheng, G. D., Lai, Y., Sun, Z., and Jiang, F.: The “thermal semiconductor” effect of crushed rocks,
544 Permafrost Periglac. Processes, 18, 151-160, 2007.
545 Cheng, G. D.: A roadbed cooling approach for the construction of Qinghai-Tibet Railway, Cold
546 Reg. Sci. Technol., 42, 169-176, 2005.
547 Cheng, G. D.: Application of thermistor in measuring permafrost temperature, Journal of
548 Glaciology and Geocryology, 2, 66-68, 1980 (in Chinese).
549 Cheng, G., and Wu, T.: Responses of permafrost to climate change and their environmental
550 significance, Qinghai-Tibet Plateau, J. Geophys. Res., 112, F02S03,
551 doi:10.1029/2006JF000631, 2007.
552 Daniel, V. M.: Thermal Variations of Mountain Permafrost: an Example of Measurements Since
553 1987 in the Swiss Alps, Global Change and Protected Areas, pp.83-95, 2001.
554 Fetter, C.W.: Applied Hydrogeology (Fourth Edition), NJ, Prentice Hall, pp.24-28, 323-326, 2000.
555 Fischer, E.M., Seneviratne, S.I., Vidale, P.L., Lüthi, D., Schär, C.: Soil moisture-atmosphere
556 interactions during the summer 2003 heatwave, J. Clim., 20, 5081-5099, 2007.
557 French, H.M.: The Periglacial Environment (Third Edition), John Wiley & Sons, Ltd., pp.38,
558 2007.
559 Gary, P., Axel, P.V.B, Amber, J.M.C.: Effect of Tillage on Soil Water Content and Temperature
560 Under Freeze-Thaw Conditions, Vadose Zone Journal, doi:10.2136/vzj2012.0075, 2013.
561 Goodrich, L.E.: The influence of snow cover on the ground thermal regime, Canadian
562 Geotechnical Journal, 19, 421-432, 1982.
563 Goyanes, G., Vieira, G., Caselli, A., Cardoso,M., Marmy, A., Santos, F., Bernardo, I., Hauck, C.:
564 Local influences of geothermal anomalies on permafrost distribution in an active volcanic
565 island (Deception Island, Antarctica), Geomorphology, 225, 57-68, 2014.
566 Guglielmin, M., Vieira, G.: Permafrost and periglacial research in Antarctica: New results and
567 perspectives, Geomorphology, <http://dx.doi.org/10.1016/j.geomorph.2014.04.005>, 2014.
568 Guglielmin, M., Worland, M.R., Baio, F., Convey, P.: Permafrost and snow monitoring at Rothera
569 Point (Adelaide Island, Maritime Antarctica): Implications for rock weathering in cryotic
570 conditions, Geomorphology, <http://dx.doi.org/10.1016/j.geomorph.2014.03.051>, 2014.
571 Han, T.D., Gao, M.J., Ye, B.S., Jiao, K.Q.: Characteristic of Runoff Process of the Glacier and
572 Permafrost in the Headwaters of the Urumuqi River, Journal of Glaciology and Geocryology,
573 32(3), 573-579, 2010(In Chinese).
574 Hao, X.H., Wang, J., Che, T., Zhang, P., Liang, J., Li, H.Y., Li, Z., Bai, Y.J., Bai Y.F.: The Spatial
575 Distribution and Properties of Snow Cover in binggou Watershed, Qilian Mountains:
576 Measurement and Analysis, Journal of Glaciology and Geocryology, 31(2), 284-292, 2009(In
577 Chinese).
578 Harris, C., Vonder Mühl, D., Isaksen, K., Haeberli, W., Ludvig Sollid, J., King, L., Holmlund, P.,
579 Dramis, F., Guglielmin, M., Palacios, D.: Warming permafrost in European mountains, Global
580 and Planetary Change, 39, 215-225, doi:10.1016/j.gloplacha.2003.04.001, 2003.
581 Hinkel, K.M., and Nelson, F. E.: Spatial and temporal patterns of active layer thickness at



- 582 Circumpolar Active Layer Monitoring (CALM) sites in northern Alaska, 1975-2000, J.
583 Geophys. Res., 108(D2), 8168, doi:10.1029/2001JD000927, 2003.
- 584 Hinkel, K.M., Paetzold, F., Nelson, F.E., Bockheim J.G.: Patterns of soil temperature and moisture
585 in the active layer and upper permafrost at Barrow, Alaska: 1993-1999, Global and Planetary
586 Change, 29(3-4), 293-309, doi:10.1016/S0921-8181(01)00096-0, 2001.
- 587 Hinzman, L.D., Kane, D.L., Gieck, R.E., Everett, K.R.: Hydrologic and thermal properties of the
588 active layer in the Alaskan Arctic, Cold Reg. Sci. Technol., 19, 95-110, 1991.
- 589 Iwata, Y., Nemoto, M., Hasegawa, S., Yanai, Y., Kuwao, K., Hirota, T.: Influence of rain, air
590 temperature, and snow cover on subsequent spring-snowmelt infiltration into thin frozen soil
591 layer in northern Japan, Journal of Hydrology 401, 165-176, 2011.
- 592 Jin, H.J., Li, S. X., Cheng, G. D., Wang, S. L., and Li, X.: Permafrost and climate change in China,
593 Global and Planetary Change, 26, 387-404, 2000.
- 594 Jin, H.J., Sun, L.P., Wang, S.L., He, R.X., Lv, L.Z., Yu, S.P.: Dual Influences of Local
595 Environmental Variables on Ground Temperatures on the Interior-Eastern Qinghai-Tibet
596 Plateau (I) : Vegetation and Snow Cover, Journal of Glaciology and Geocryology, 30(4),
597 535-545, 2008(In Chinese).
- 598 Keller, F., and Gubler, H.U.: Interaction between snow cover and high mountain permafrost
599 Murtel/Corvatsch, Swiss Alps, in Proceedings of the 6th International Conference on
600 Permafrost, Beijing, pp. 332-337, 1993.
- 601 Kunio, W. and Tomomi, W.: Measurement of unfrozen water content and relative permittivity of
602 frozen unsaturated soil using NMR and TDR, Cold Regions Science and Technology, 59,
603 34-41, 2009.
- 604 Lemke, P., Ren, J., Alley, R.B., Allison, I., Carrasco, J., Flato, G., Fujii, Y., Kaser, G., Mote, P.,
605 Thomas, R.H. and Zhang, T.J.: Observations: Changes in snow, ice and frozen ground, in
606 Climate Change 2007: The Physical Science Basis. Contribution of Working Group I to the
607 Fourth Assessment Report of the Intergovernmental Panel on Climate Change, edited by S.
608 Solomon et al., pp. 369-374, Cambridge Univ. Press, Cambridge, U. K, 2007.
- 609 Li, J., Sheng, Y., Chen, J., Wu, J.C., Wang, S.T.: Variations in Permafrost Temperature and
610 Stability of Alpine Meadows in the Source Area of the Datong River, Northeastern
611 Qinghai-Tibet Plateau, China, Permafrost and Periglacial Processes, 307-319, DOI:
612 10.1002/ppp.1822, 2014.
- 613 Li, J., Sheng, Y., Wu, J.C., Wang, J., Zhang, B., Ye, B.S., Zhang X.M., Qin, X.: Modeling
614 Regional and Local-scale Permafrost Distribution in Qinghai-Tibet Plateau Using
615 Equivalent-elevation Method, Chinese Geografical Science, 22(3), 278-287, 2012.
- 616 Liang, L.H., Zhou, Y.W.: The Characteristics of the Distribution of Snow Cover and its Warm
617 Effect of the Temperature of Permafrost, Amuer Region, Da Hinggan Ling, China,
618 Proceedings of SICOP, Beijing, China, 393-396, 1993.
- 619 Ling, F., and Zhang, T.J.: Impact of the Timing and Duration of Seasonal Snow Cover on the
620 Active Layer and Permafrost in the Alaskan Arctic, Permafrost Periglac. Process., 14, 141-150,
621 2003.
- 622 Ling, F., and Zhang, T.J.: Sensitivity of ground thermal regime and surface energy fluxes to tundra
623 snow density in northern Alaska, Cold Regions Science and Technology, 44, 121-130, 2006.
- 624 Liu, J.M., Shen, Y., Zhao, S.P.: High-Precision Thermistor Temperature Sensor: Technological
625 Improvement and Application, Journal of Glaciology and Geocryology, 33(4), 765-771, 2011..



- 626 Luetschg, M., Lehning, M., Haeberli, W.: A sensitivity study of factors influencing warm/thin
627 permafrost in the Swiss Alps, *Journal of Glaciology*, 54(187), 696-704, 2008.
- 628 Lv Y.C.: The experience of land reclamation in Delingha city, *Soils*, (5), 24-25, 1960 (In
629 Chinese).
- 630 Morin S., Domine, F., Arnaud, L., Picard, G.: In-situ monitoring of the time evolution of the
631 effective thermal conductivity of snow, *Cold Regions Science and Technology*, 64(2), 73-80.
632 doi:10.1016/j.coldregions.2010.02.008, 2010.
- 633 Muller, S.W.: Permafrost or Permanently Frozen Ground and Related Engineering Problems,
634 Edwards, Ann Arbor, Mich, 1947.
- 635 Neal, J.H.: The Effect of the Degree of Slope and Rainfall Characteristics on Runoff and Soil
636 Erosion, *Soil Science Society of America Journal*, 2(c), 525-532, 1938.
- 637 Nelson, F. E., Shiklomanov, N. I., Hinkel, K. M. and Christiansen, H.H.: The Circumpolar Active
638 Layer Monitoring (CALM) Workshop and the CALM II Program, *International Permafrost
639 Assoc.*, *Polar Geogr.*, 28, 253-266, doi:10.1080/789610205, 2004.
- 640 Penman, H.L.: Natural Evaporation from Open Water, Bare Soil and Grass, *Proc. R. Soc. Lond. A*
641 1948, 193, 120-145. doi: 10.1098/rspa.1948.0037, 1948.
- 642 Reimer, A.: The effect of wind on heat transfer in snow, *Cold Reg. Sci. Technol.*, 3(2-3), 129-137,
643 1980.
- 644 Shen, Y., Liu, J.M., Zhao S.P.: Long-term Stability of Thermometric Thermistor Sensor
645 SKLFSE-TS Used at Low Temperature, *Journal of Glaciology and Geocryology*, 2012, 34(4),
646 891-897, 2012 (in Chinese).
- 647 Smith, M.W.: Microclimatic influences on ground temperatures and permafrost distribution,
648 Mackenzie Delta, Northwest Territories, *Canadian Journal of Earth Sciences*, 12, 1421-1438,
649 1975.
- 650 Sturm, M. and Johnson, J.B.: Thermal conductivity measurements of depth hoar, *J. Geophys. Res.*,
651 97(B2), 2129-2139, 1992.
- 652 Sturm, M., Holmgren, J., Konig, M. and Morris K.: The thermal conductivity of seasonal snow, *J.
653 Glaciol.*, 43, 26-41, 1997.
- 654 Sun, Y.H., Huang, X.D., Wang, W.: Spatio-temporal changes of snow cover and snow water
655 equivalent in the Tibetan Plateau during 2003-2010, *Journal of Glaciology and Geocryology*,
656 36(6), 1337-1344, Doi:10.7522/j.issn.1000-0240.2014.0160, 2014 (in Chinese).
- 657 Tobias, R., Christof, K.: Influence of snow cover and grain size on the ground thermal regime in
658 the discontinuous permafrost zone, Swiss Alps, *Geomorphology*, 176-189,
659 doi:10.1016/j.geomorph.2012.07.008, 2012.
- 660 Tong, B.L., Li, S.D., Zhang, T.J.: Frozen ground in the Altay Mountains of China, *Journal of
661 Glaciology and Geocryology*, 8(4), 357-364, 1986 (in Chinese).
- 662 Wang, G.X., Hu, H.C., Li, T.B.: The influence of freeze-thaw cycles of active soil layer on surface
663 runoff in a permafrost watershed, *Journal of Hydrology*, 375(3-4), 438-449, 2009.
- 664 Wang, S., Guo, H.Y.: Temperature responses to climate changes in western Qilian desert
665 transition edge, *Journal of Lanzhou University (Natural Sciences)*, 49(3), 332-336, 2013.
- 666 Wang, Z.L., Fu, Q., Jiang, Q.X., Li, T.X.: Numerical simulation of water-heat coupled movements
667 in seasonal frozen soil, *Mathematical and Computer Modelling*, 54, 970-975, 2011.
- 668 Washburn, A.L.: *Geocryology: A Survey of Periglacial Processes and Environments*, Edward
669 Arnold, Londres, 1979.



- 670 Weller, G., Holmgren, B.: The microclimates of The Arctic tundra, Journal of Applied
671 Meteorology, 13 (8), 854- 862, 1974.
- 672 Williams, P.J., Smith, M.W.: The Frozen Earth: Fundamentals of Geocryology, Cambridge Univ.
673 Press, Cambridge, pp. 306, 1989.
- 674 Wu, Q.B. and Liu, Y.Z.: Ground temperature monitoring and its recent change in Qinghai- Tibet
675 Plateau, Cold Reg. Sci. Technol., 38, 85-92, doi:10.1016/S0165-232X(03)00064-8, 2004.
- 676 Wu, Q.B. and Zhang, T.J.: Changes in Active Layer Thickness over the Qinghai-Tibetan Plateau
677 from 1995-2007, J. Geophys. Res., 115, D09107, doi:10.1029/2009JD01297, 2010.
- 678 Wu, Q.B. and Zhang, T.J.: Recent Permafrost Warming on the Qinghai-Tibetan Plateau, J.
679 Geophys. Res., 11, D13108, doi:10.1029/2007JD009539, 2008.
- 680 Wu, Q.B., Zhang, T.J., and Liu, Y.Z.: Thermal State of the Active Layer and Permafrost along the
681 Qinghai-Xizang(Tibet) Railway from 2006 to 2010, The Cryosphere, 6, 607-612, 2012.
- 682 Xiang, X.H., Wu, X.L., Wang, C.H., Chen X., Shao, Q.Q.: Influences of climate variation on
683 thawing-freezing processes in the northeast of Three-River Source Region China, Cold
684 Regions Science and Technology, 86, 86-97, 2013.
- 685 Yeh, T.C., Wetherald, R.T. and Manabe, S.: A Model Study of the Short-Term Climatic and
686 Hydrologic Effects of Sudden Snow-Cover Removal, Mon. Wea. Rev., 111(5), 1013-1024.
687 doi: [http://dx.doi.org/sci-hub.org/10.1175/1520-0493\(1983\)1112.0.](http://dx.doi.org/sci-hub.org/10.1175/1520-0493(1983)1112.0.), 1983.
- 688 Yen, Y.C.: Effective thermal conductivity and water vapor diffusivity of naturally compacted
689 snow, J. Geophys. Res., 70(8), 1821-1825, 1965.
- 690 Yershov, E.D.: General Geocryology, Cambridge University Press, Cambridge, 1998.
- 691 Zeng, Q.Z., Zhang, S.Y., Jin, D.H.: Satellite Monitoring of Snow cover in Qilian Mountain and
692 Analysis on Snowmelt Runoff in Hexi district, Journal of Glaciology and Geocryology, 7(1),
693 295-304, 1985 (In Chinese).
- 694 Zhang, T.J., Osterkamp, T.E. and Stamnes, K.: Influence of the Depth Hoar Layer of the Seasonal
695 Snow Cover on the Ground Thermal Regime, Water Resour. Res., 32(7), 2075-2086, 1996.
- 696 Zhang, T.J., Frauenfeld, O.W., Serreze, M.C., Etringer, A., Oelke, C.: Spatial and temporal
697 variability in active layer thickness over the Russian Arctic drainage basin, J. Geophys. Res.,
698 110, D16101, doi:10.1029/2004JD005642, 2005.
- 699 Zhang, T.J.: Influence of the seasonal snow cover on the ground thermal regime: An overview,
700 Rev. Geophys., 43, RG4002,1-23, 2005.
- 701 Zhao, L., Cheng, G.D., and Li, S.H.: Thawing and freezing processes of active layer in
702 Wudaoliang region of Tibetan Plateau, Chinese Sci. Bull., 45, 2181-2186, 2000.
- 703 Zhao, L., Ping, C., Yang, D., Cheng, G., Ding, Y. and Liu, S.: Changes of climate and seasonally
704 frozen ground over the past 30years in Qinghai-Xizang (Tibetan) Plateau, China, Global Planet.
705 Change, 43, 19-31, 2004.
- 706 Zhao, L., Wu, Q. B., Marchenko, S.S. and Sharkhuu, N.: Thermal state of Permafrost and active
707 layer in Central Asia during the International Polar Year, Permafrost and Periglac. Process, 21,
708 198-207, 2010.
- 709 Zhao, L., Wu, T., Ding, Y., and Xie, C.W.: Monitoring permafrost changes on the Qinghai-Tibet
710 Plateau, in: Extended Abstracts, Proceedings of the Ninth International Conference on
711 Permafrost, vol. 2, edited by: Kane D. L and Hinkel, K. M., Institute of Northern Engineering,
712 University of Alaska, Fairbanks, Alaska, 2071-2076, 2008.
- 713 Zhou J., Wolfgang, I., Cheng, G.D., Zhang, W., He, X.B., Ye, B.S.: Monitoring and modeling the



714 influence of snow pack and organic soil on a permafrost active layer, Qinghai-Tibetan Plateau
715 of China, Cold Regions Science and Technology, 90-91, 38-52, 2013.